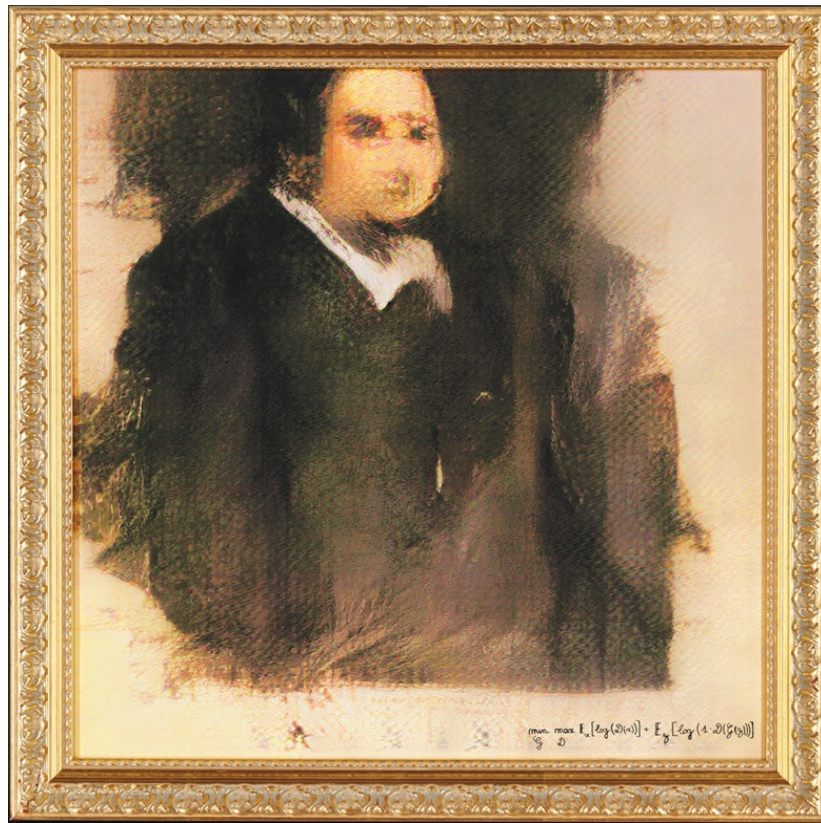


Deep Learning

Lecture 11: Generative adversarial networks

Prof. Gilles Louppe
g.louppe@uliege.be





*"Generative adversarial networks is the coolest idea
in deep learning in the last 20 years."*

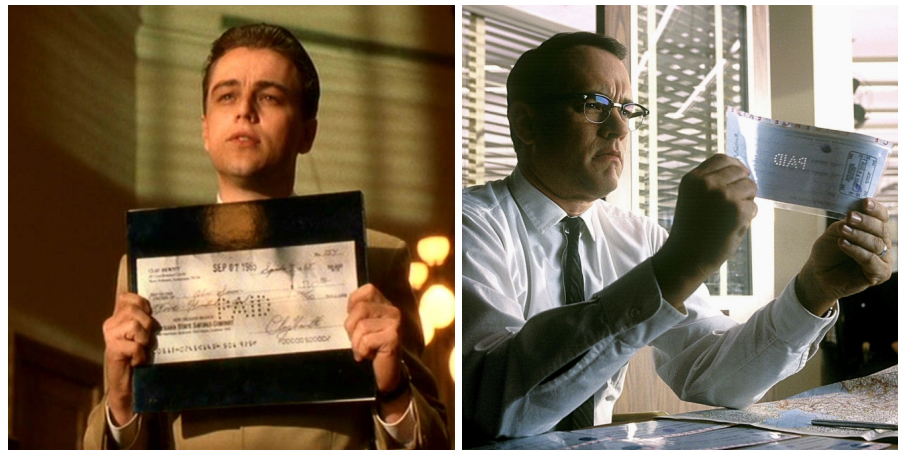
Yann LeCun, 2018.

Today

Learn a model of the data.

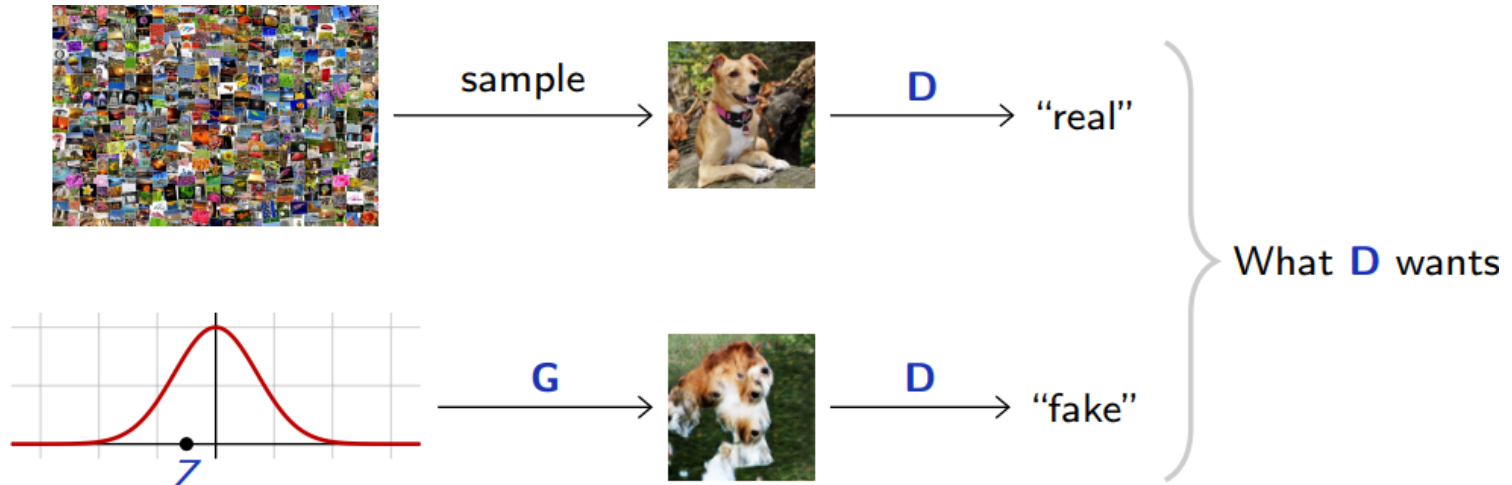
- Generative adversarial networks
- Numerics of GANs
- State of the art
- Applications

Generative adversarial networks



A two-player game

In **generative adversarial networks** (GANs), the task of learning a generative model is expressed as a two-player zero-sum game between two networks.



The first network is a **generator** $g(\cdot; \theta) : \mathcal{Z} \rightarrow \mathcal{X}$, mapping a latent space equipped with a prior distribution $p(\mathbf{z})$ to the data space, thereby inducing a distribution

$$\mathbf{x} \sim q(\mathbf{x}; \theta) \Leftrightarrow \mathbf{z} \sim p(\mathbf{z}), \mathbf{x} = g(\mathbf{z}; \theta).$$

The second network $d(\cdot; \phi) : \mathcal{X} \rightarrow [0, 1]$ is a **classifier** trained to distinguish between true samples $\mathbf{x} \sim p(\mathbf{x})$ and generated samples $\mathbf{x} \sim q(\mathbf{x}; \theta)$.

For a fixed generator \mathbf{g} , the classifier \mathbf{d} can be trained by generating a two-class training set

$$\mathbf{d} = \{(\mathbf{x}_1, y=1), \dots, (\mathbf{x}_N, y=1), (g(\mathbf{z}_1; \theta), y=0), \dots, (g(\mathbf{z}_N; \theta), y=0)\},$$

where $\mathbf{x}_i \sim p(\mathbf{x})$ and $\mathbf{z}_i \sim p(\mathbf{z})$, and minimizing the cross-entropy loss

$$\begin{aligned}\mathcal{L}(\phi) &= -\frac{1}{2N} \sum_{i=1}^N [\log d(\mathbf{x}_i; \phi) + \log (1 - d(g(\mathbf{z}_i; \theta); \phi))] \\ &\approx -\mathbb{E}_{\mathbf{x} \sim p(\mathbf{x})} [\log d(\mathbf{x}; \phi)] - \mathbb{E}_{\mathbf{z} \sim p(\mathbf{z})} [\log(1 - d(g(\mathbf{z}; \theta); \phi))].\end{aligned}$$

However, the situation is slightly more complicated since we also want to train \mathbf{g} to fool the discriminator. Fortunately, this is equivalent to maximizing \mathbf{d} 's loss.

Let us consider the **value function**

$$V(\phi, \theta) = \mathbb{E}_{\mathbf{x} \sim p(\mathbf{x})} [\log d(\mathbf{x}; \phi)] + \mathbb{E}_{\mathbf{z} \sim p(\mathbf{z})} [\log(1 - d(g(\mathbf{z}; \theta); \phi))].$$

- For a fixed g , $V(\phi, \theta)$ is high if d is good at recognizing true from generated samples.
- If d is the best classifier given g , and if V is high, then this implies that the generator is bad at reproducing the data distribution.
- Conversely, g will be a good generative model if V is low when d is a perfect opponent.

Therefore, the ultimate goal is

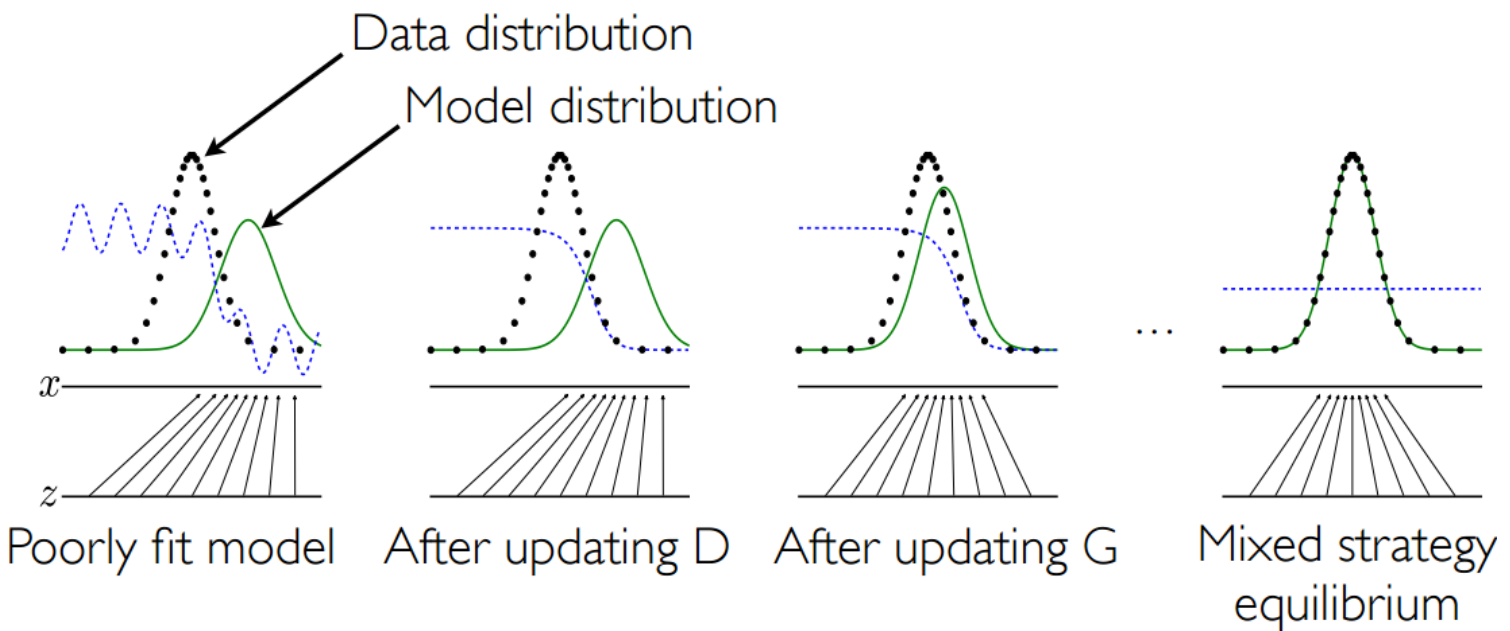
$$\theta^* = \arg \min_{\theta} \max_{\phi} V(\phi, \theta).$$

Learning process

In practice, the minimax solution is approximated using [alternating](#) stochastic gradient descent:

$$\begin{aligned}\theta &\leftarrow \theta - \gamma \nabla_{\theta} V(\phi, \theta) \\ \phi &\leftarrow \phi + \gamma \nabla_{\phi} V(\phi, \theta),\end{aligned}$$

where gradients are estimated with Monte Carlo integration.



Game analysis

For a generator \mathbf{g} fixed at θ , the classifier d with parameters ϕ_θ^* is optimal if and only if

$$\forall \mathbf{x}, d(\mathbf{x}; \phi_\theta^*) = \frac{p(\mathbf{x})}{q(\mathbf{x}; \theta) + p(\mathbf{x})}.$$

Therefore,

$$\begin{aligned} \min_{\theta} \max_{\phi} V(\phi, \theta) &= \min_{\theta} V(\phi_{\theta}^*, \theta) \\ &= \min_{\theta} \mathbb{E}_{\mathbf{x} \sim p(\mathbf{x})} \left[\log \frac{p(\mathbf{x})}{q(\mathbf{x}; \theta) + p(\mathbf{x})} \right] + \mathbb{E}_{\mathbf{x} \sim q(\mathbf{x}; \theta)} \left[\log \frac{q(\mathbf{x}; \theta)}{q(\mathbf{x}; \theta) + p(\mathbf{x})} \right] \\ &= \min_{\theta} \text{KL} \left(p(\mathbf{x}) \parallel \frac{p(\mathbf{x}) + q(\mathbf{x}; \theta)}{2} \right) \\ &\quad + \text{KL} \left(q(\mathbf{x}; \theta) \parallel \frac{p(\mathbf{x}) + q(\mathbf{x}; \theta)}{2} \right) - \log 4 \\ &= \min_{\theta} 2 \text{JSD}(p(\mathbf{x}) || q(\mathbf{x}; \theta)) - \log 4 \end{aligned}$$

where **JSD** is the Jensen-Shannon divergence.

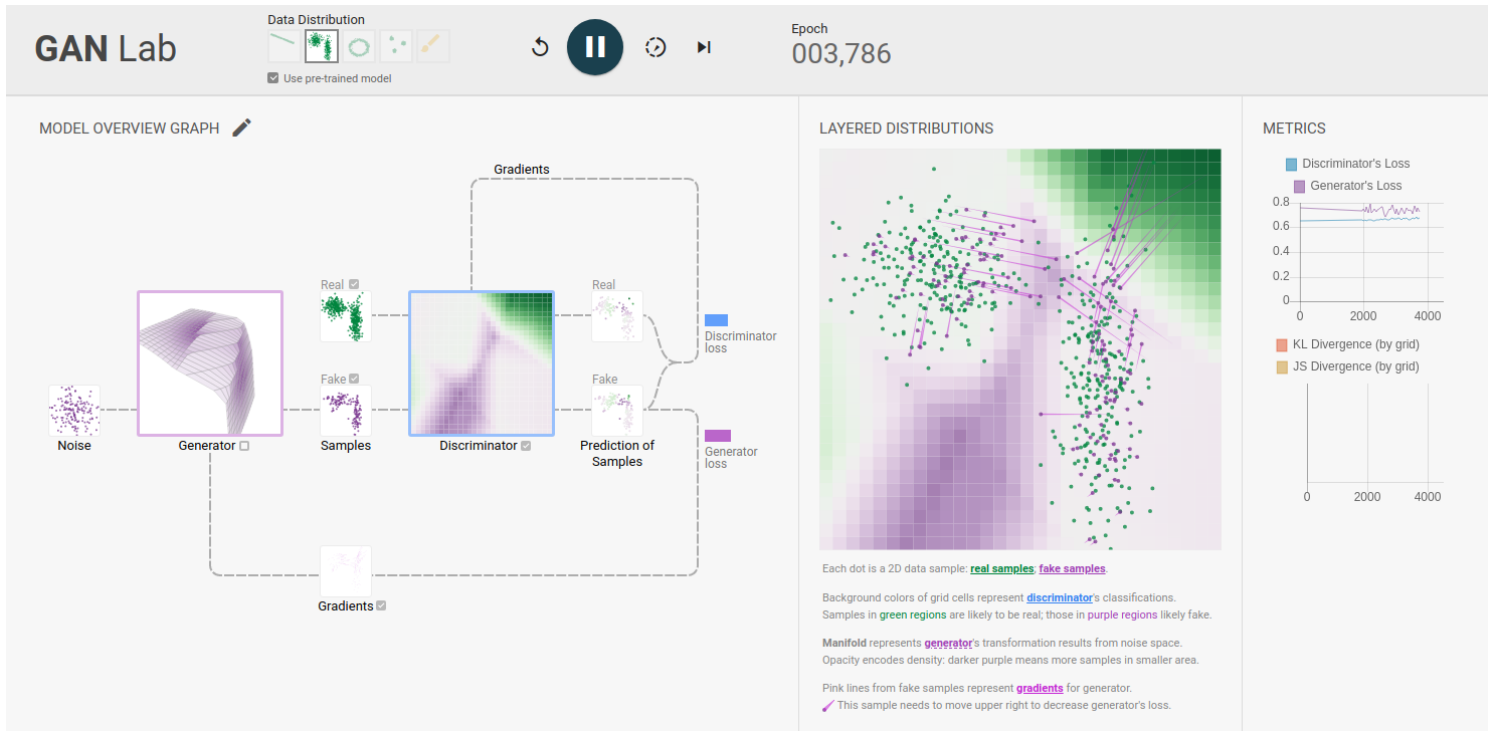
In summary,

$$\begin{aligned}\theta^* &= \arg \min_{\theta} \max_{\phi} V(\phi, \theta) \\ &= \arg \min_{\theta} \text{JSD}(p(\mathbf{x}) || q(\mathbf{x}; \theta)).\end{aligned}$$

Since $\text{JSD}(p(\mathbf{x}) || q(\mathbf{x}; \theta))$ is minimum if and only if

$$p(\mathbf{x}) = q(\mathbf{x}; \theta)$$

for all \mathbf{x} , this proves that the minimax solution corresponds to a generative model that perfectly reproduces the true data distribution.



(demo)

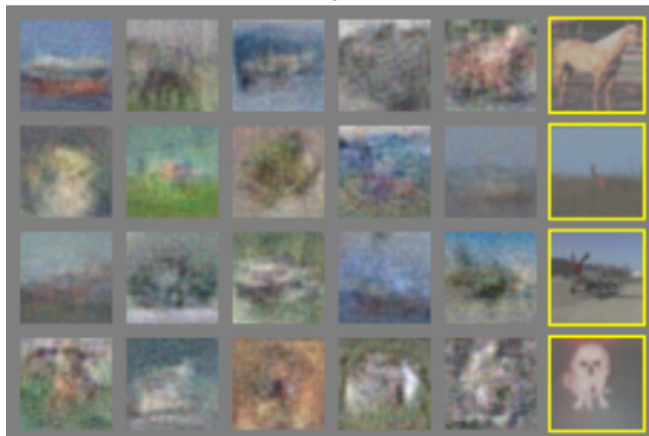
Results



a)



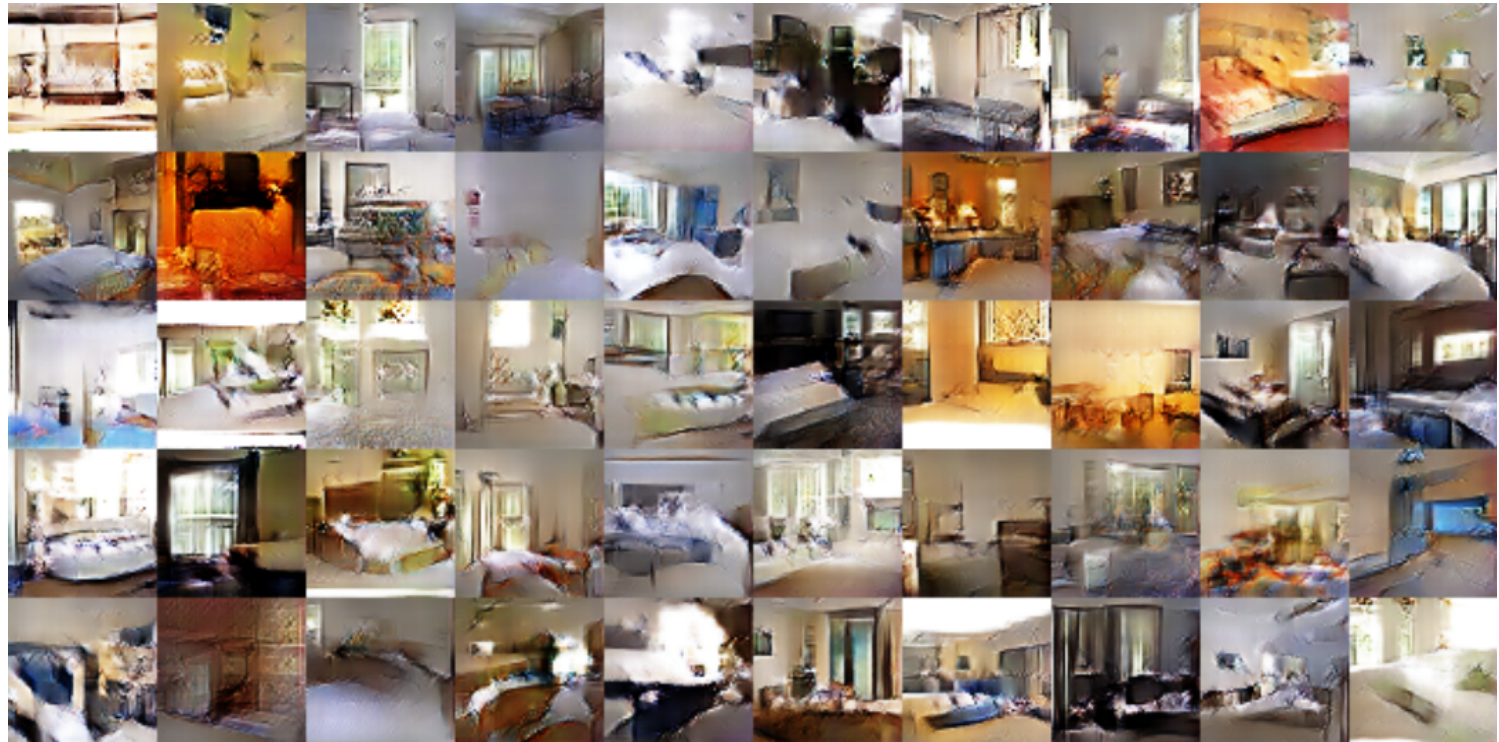
b)

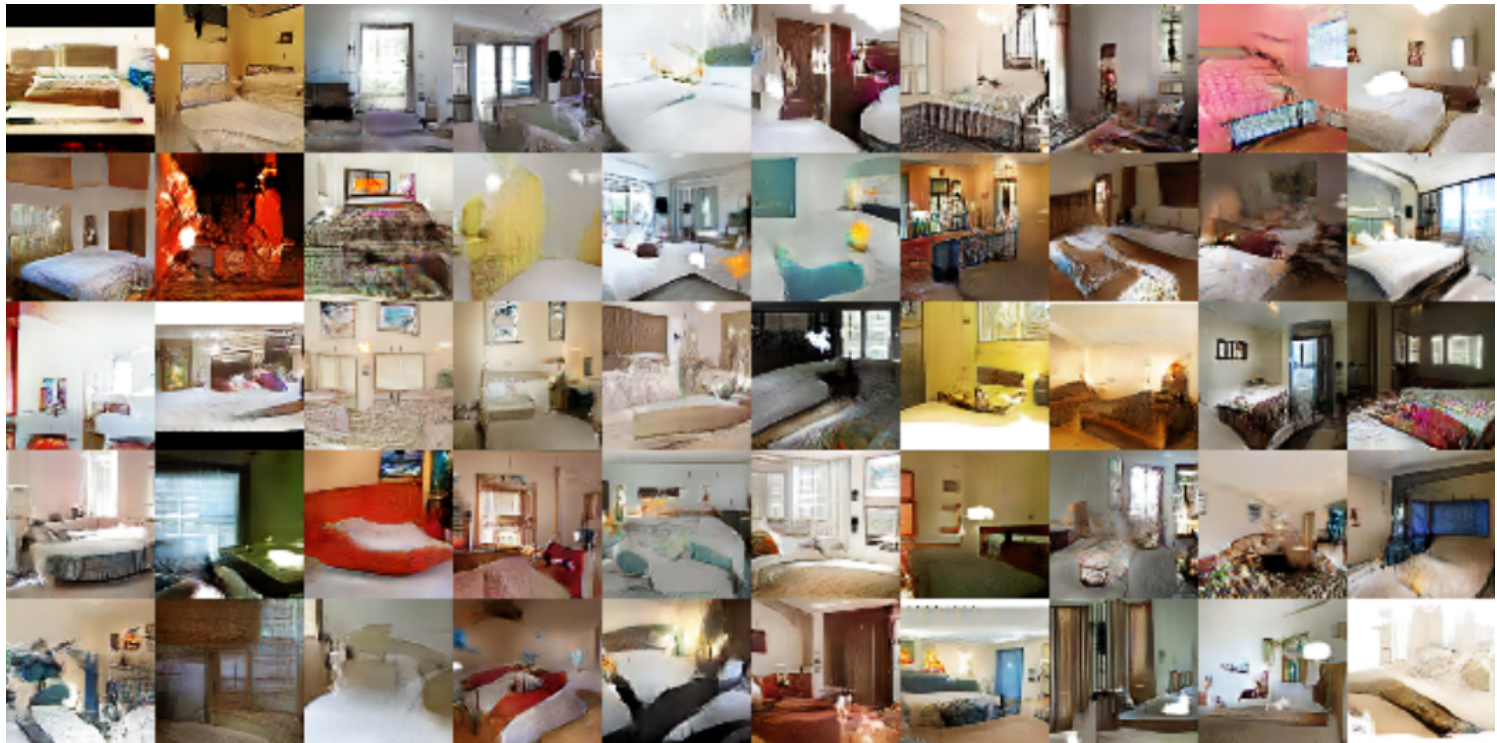


c)



d)

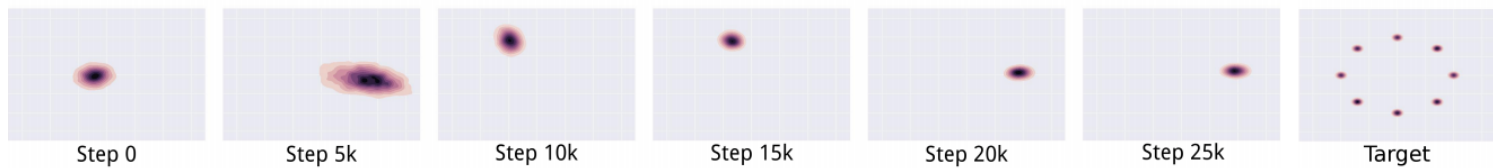




Open problems

Training a standard GAN often results in pathological behaviors:

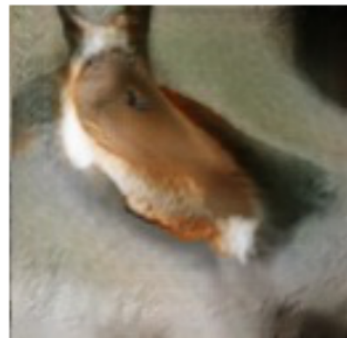
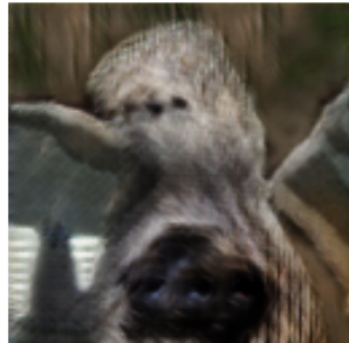
- **Oscillations** without convergence: contrary to standard loss minimization, alternating stochastic gradient descent has no guarantee of convergence.
- **Vanishing gradients**: when the classifier d is too good, the value function saturates and we end up with no gradient to update the generator.
- **Mode collapse**: the generator g models very well a small sub-population, concentrating on a few modes of the data distribution.
- Performance is also difficult to assess in practice.



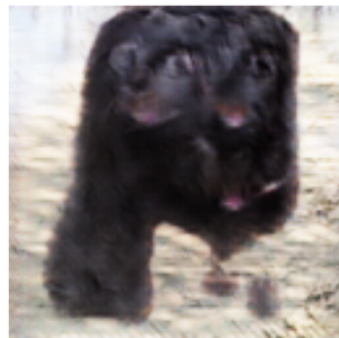
Mode collapse (Metz et al, 2016)

Cabinet of curiosities

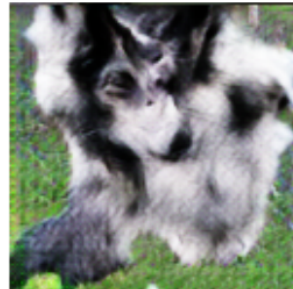
While early results (2014-2016) were already impressive, a close inspection of the fake samples distribution $q(\mathbf{x}; \theta)$ often revealed fundamental issues highlighting architectural limitations.



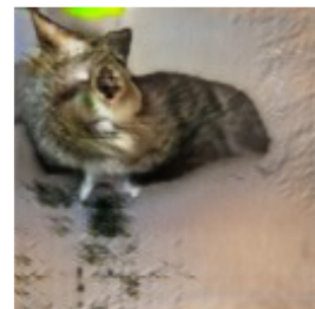
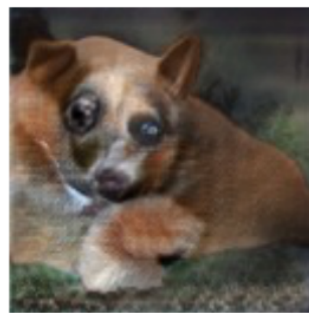
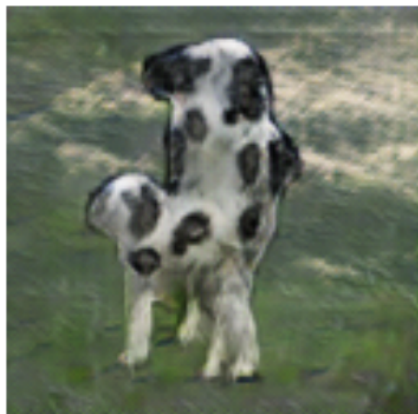
Cherry-picks



Problems with counting

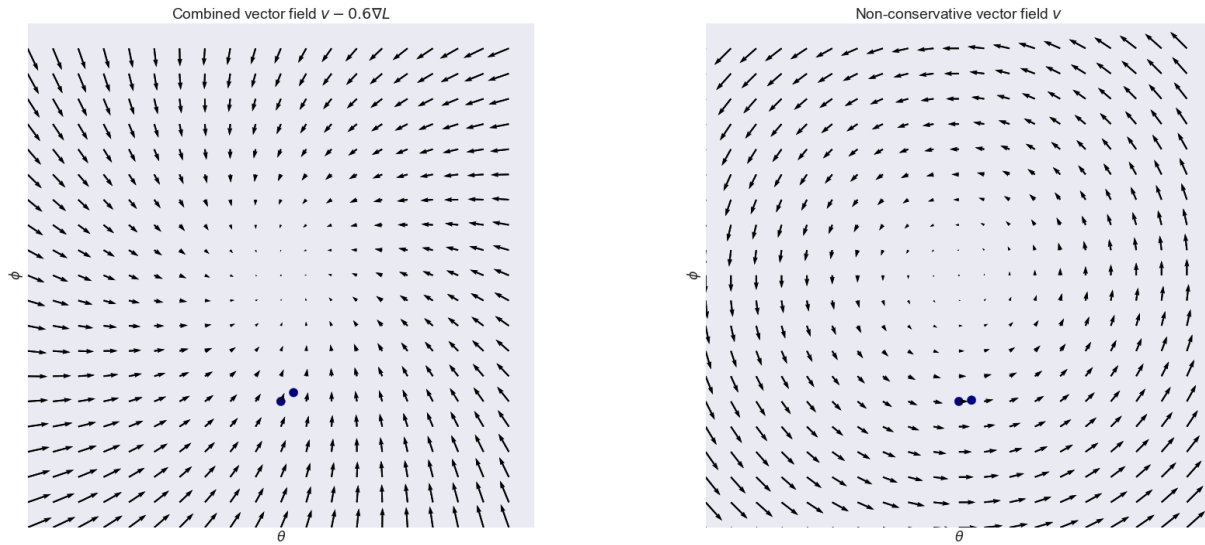


Problems with perspective



Problems with global structures

Numerics of GANs



Solving for saddle points is different from gradient descent.

- Minimization of scalar functions yields **conservative** vector fields.
- Min-max saddle point problems may yield **non-conservative** vector fields.

Following the notations of Mescheder et al (2018), the training objective for the two players can be described by an objective function of the form

$$L(\theta, \phi) = \mathbb{E}_{p(\mathbf{z})} [f(d(g(\mathbf{z}; \theta); \phi))] + \mathbb{E}_{p(\mathbf{x})} [f(-d(\mathbf{x}; \phi))],$$

where the goal of the generator is to minimizes the loss, whereas the discriminator tries to maximize it.

If $f(t) = -\log(1 + \exp(-t))$, then we recover the original GAN objective (assuming that d outputs the logits).

Training algorithms can be described as fixed points algorithms that apply some operator $F_h(\theta, \phi)$ to the parameters values (θ, ϕ) .

- For simultaneous gradient descent,

$$F_h(\theta, \phi) = (\theta, \phi) + h v(\theta, \phi)$$

where $v(\theta, \phi)$ denotes the **gradient vector field**

$$v(\theta, \phi) := \begin{pmatrix} -\frac{\partial L}{\partial \theta}(\theta, \phi) \\ \frac{\partial L}{\partial \phi}(\theta, \phi) \end{pmatrix}$$

and h is a scalar stepsize.

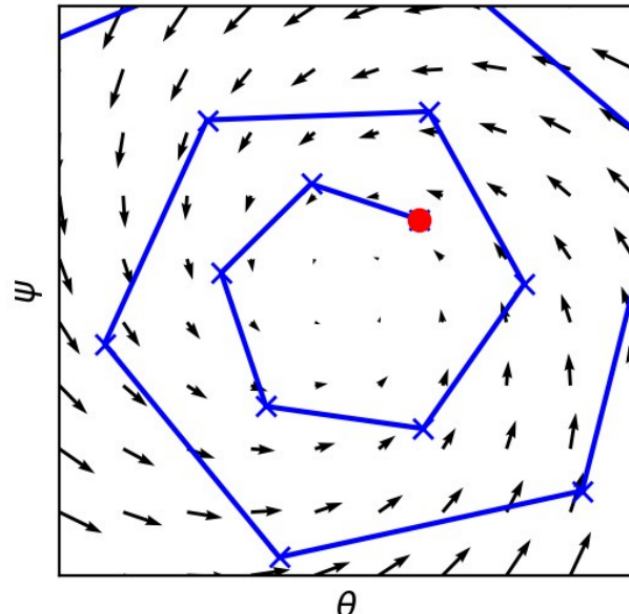
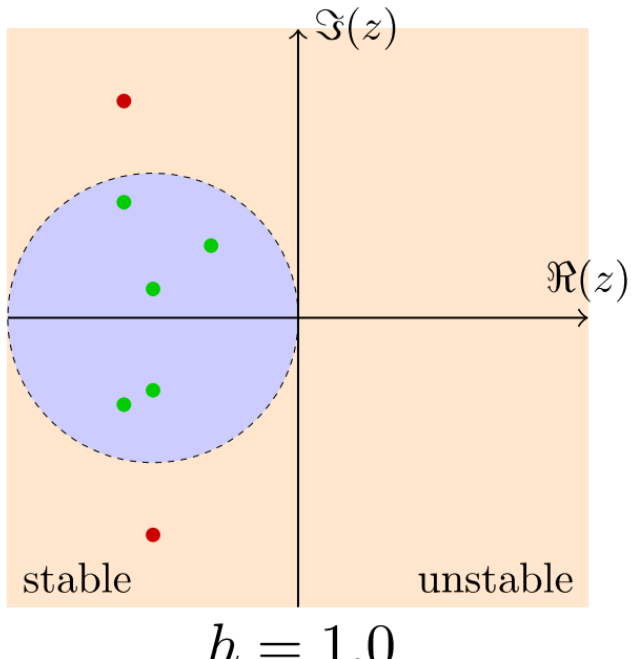
- Similarly, alternating gradient descent can be described by an operator $F_h = F_{2,h} \circ F_{1,h}$, where $F_{1,h}$ and $F_{2,h}$ perform an update for the generator and discriminator, respectively.

Local convergence near an equilibrium point

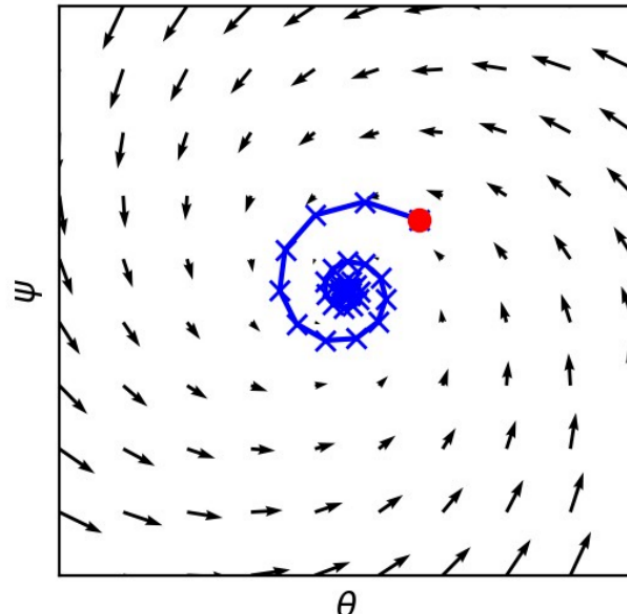
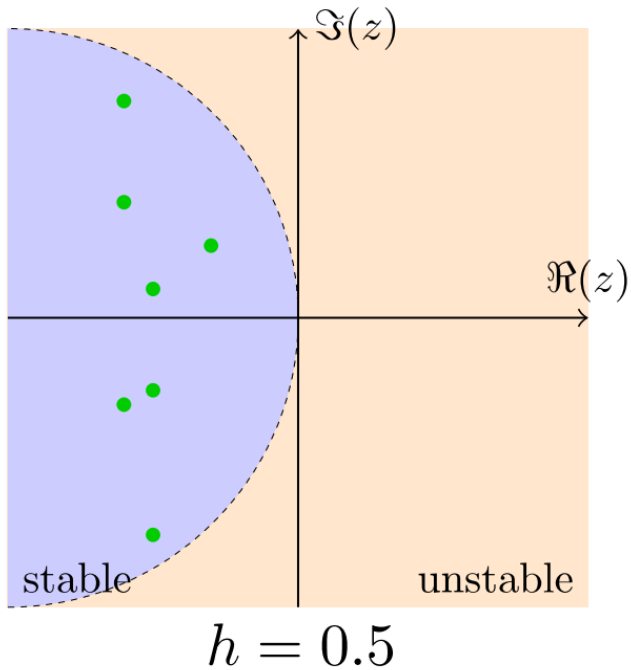
Let us consider the Jacobian $J_{F_h}(\theta^*, \phi^*)$ at the equilibrium (θ^*, ϕ^*) :

- if $J_{F_h}(\theta^*, \phi^*)$ has eigenvalues with absolute value bigger than 1, the training will generally not converge to (θ^*, ϕ^*) .
- if all eigenvalues have absolute value smaller than 1, the training will converge to (θ^*, ϕ^*) .
- if all eigenvalues values are on the unit circle, training can be convergent, divergent or neither.

Mescheder et al (2017) show that all eigenvalues can be forced to remain within the unit ball if and only if the stepsize h is made sufficiently small.



Discrete system: divergence ($h = 1$, too large).



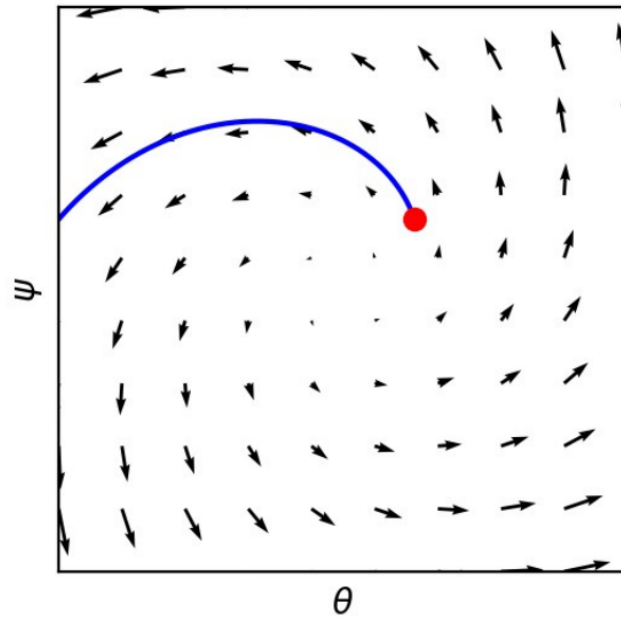
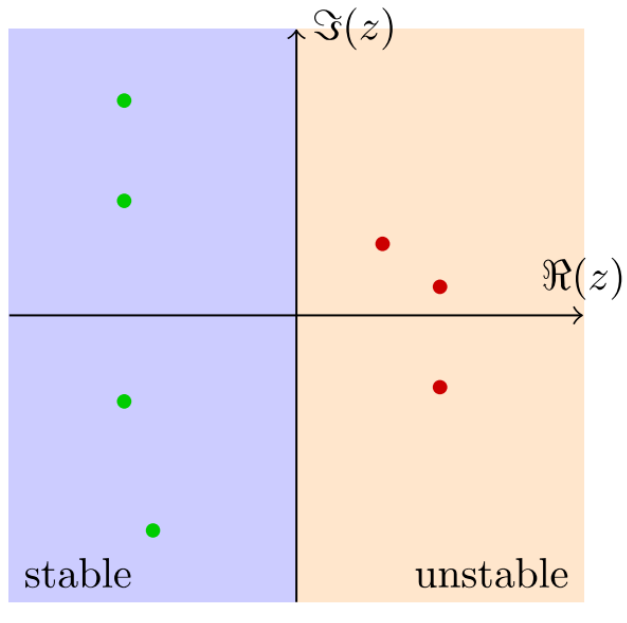
Discrete system: convergence ($h = 0.5$, small enough).

For the (idealized) continuous system

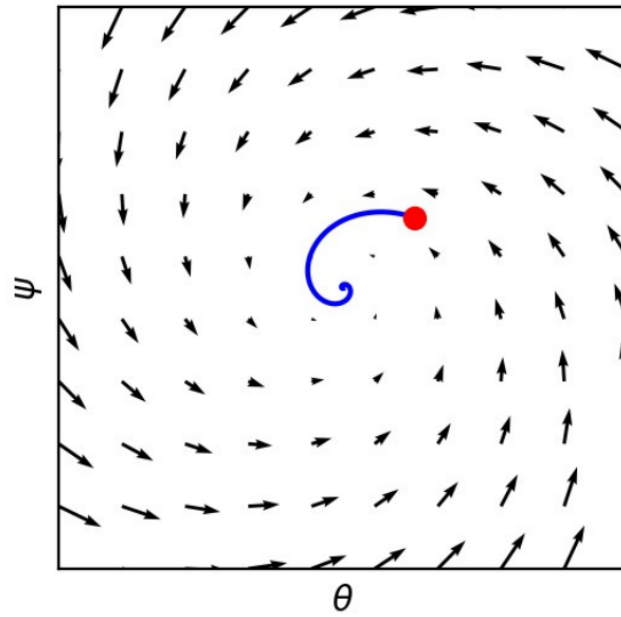
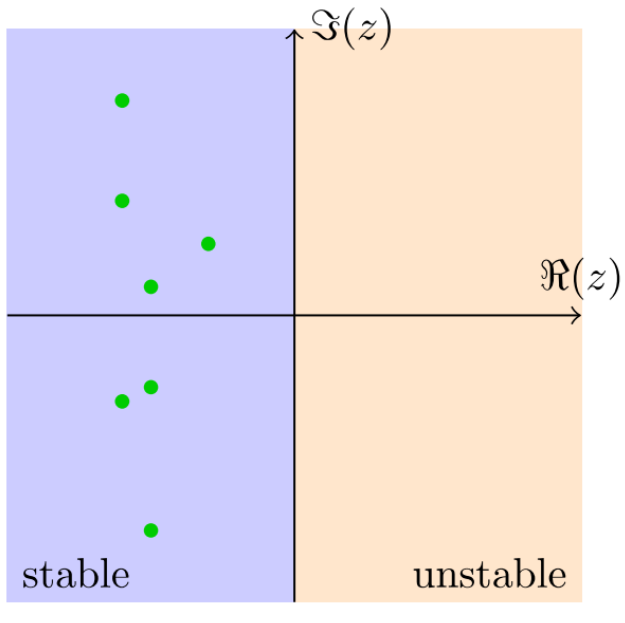
$$\begin{pmatrix} \dot{\theta}(t) \\ \dot{\phi}(t) \end{pmatrix} = \begin{pmatrix} -\frac{\partial L}{\partial \theta}(\theta, \phi) \\ \frac{\partial L}{\partial \phi}(\theta, \phi) \end{pmatrix},$$

which corresponds to training GANs with infinitely small learning rate $h \rightarrow 0$:

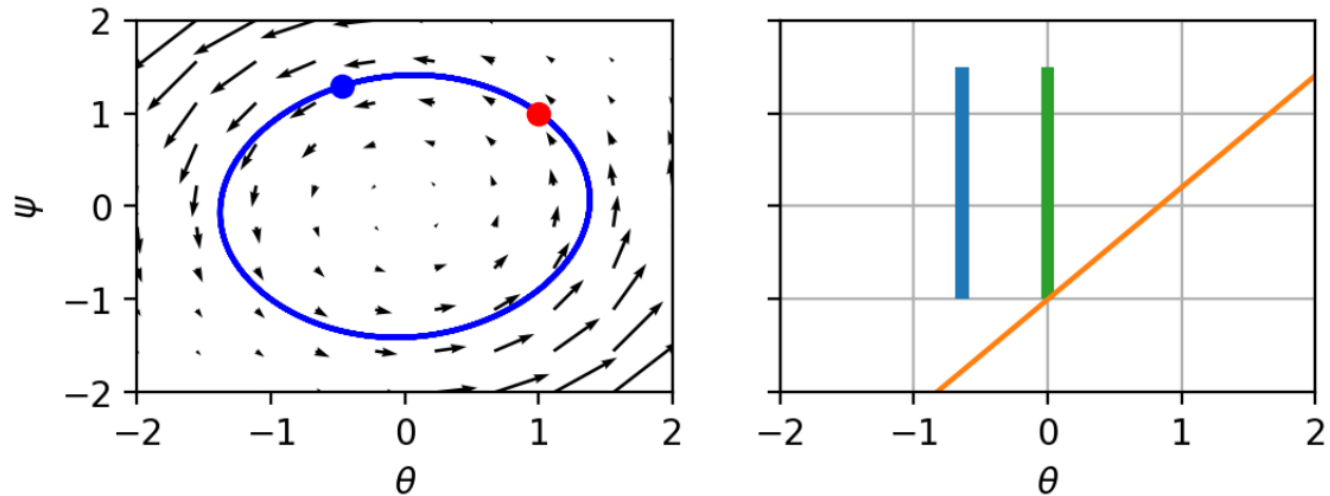
- if all eigenvalues of the Jacobian $v'(\theta^*, \phi^*)$ at a stationary point (θ^*, ϕ^*) have negative real-part, the continuous system converges locally to (θ^*, ϕ^*) ;
- if $v'(\theta^*, \phi^*)$ has eigenvalues with positive real-part, the continuous system is not locally convergent.
- if all eigenvalues have zero real-part, it can be convergent, divergent or neither.



Continuous system: divergence.

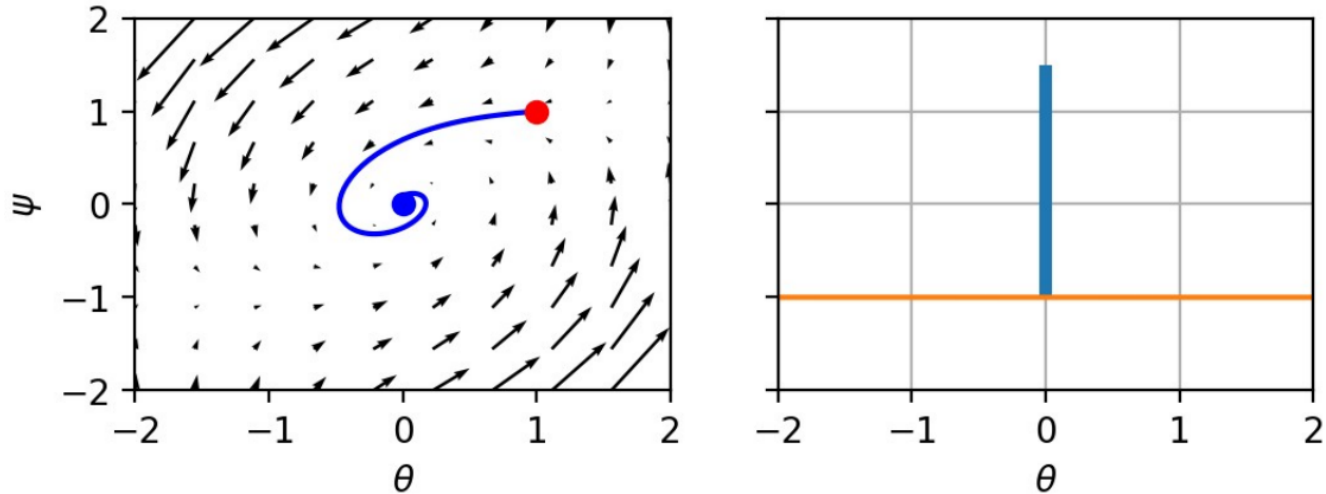


Continuous system: convergence.



On the Dirac-GAN toy problem, eigenvalues are $\{-f'(0)i, +f'(0)i\}$. Therefore convergence of the standard GAN learning procedure is not guaranteed.

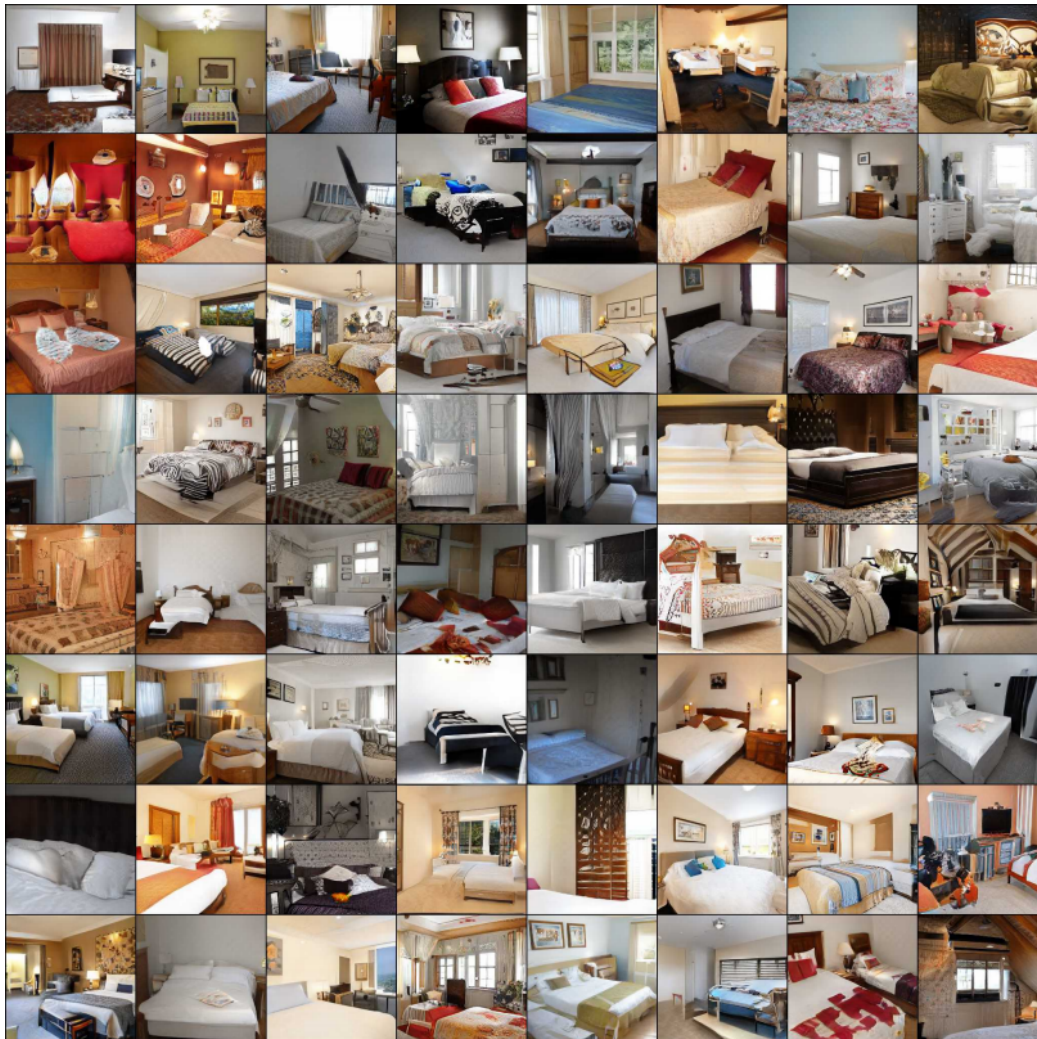
Taming the vector field



A penalty on the squared norm of the gradients of the discriminator results in the regularization

$$R_1(\phi) = \frac{\gamma}{2} \mathbb{E}_{\mathbf{x} \sim p(\mathbf{x})} [||\nabla_{\mathbf{x}} d(\mathbf{x}; \phi)||^2].$$

The resulting eigenvalues are $\{-\frac{\gamma}{2} \pm \sqrt{\frac{\gamma}{4} - f'(0)^2}\}$. Therefore, for $\gamma > 0$, all eigenvalues have negative real part, hence training is locally convergent!







State of the art



Ian Goodfellow

@goodfellow_ian

4.5 years of GAN progress on face generation. arxiv.org/abs/1406.2661

arxiv.org/abs/1511.06434

arxiv.org/abs/1606.07536

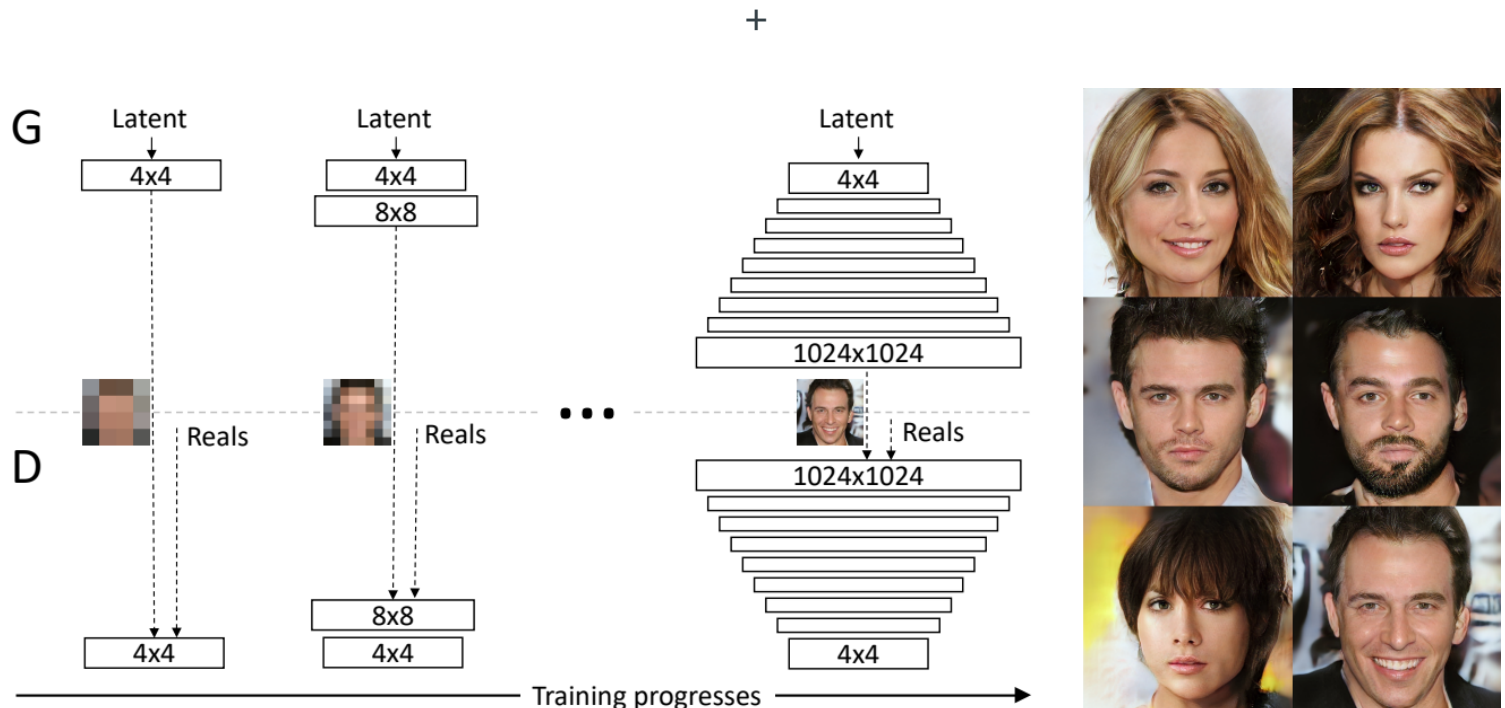
arxiv.org/abs/1710.10196

arxiv.org/abs/1812.04948



Progressive growing of GANs

Wasserstein GANs as baseline (Arjovsky et al, 2017) +
Gradient Penalty (Gulrajani, 2017) + (quite a few other tricks)



(Karras et al, 2017)

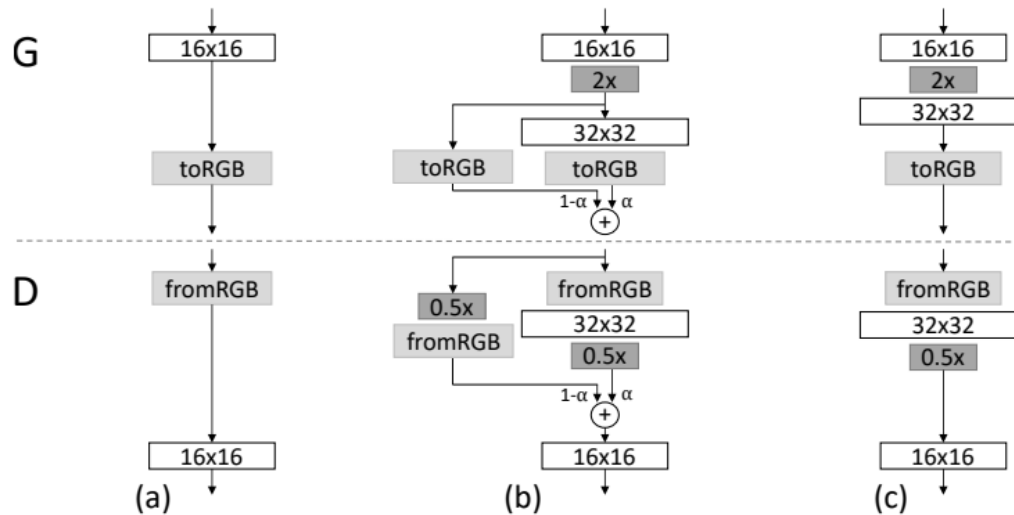


Figure 2: When doubling the resolution of the generator (G) and discriminator (D) we fade in the new layers smoothly. This example illustrates the transition from 16×16 images (a) to 32×32 images (c). During the transition (b) we treat the layers that operate on the higher resolution like a residual block, whose weight α increases linearly from 0 to 1. Here $2\times$ and $0.5\times$ refer to doubling and halving the image resolution using nearest neighbor filtering and average pooling, respectively. The toRGB represents a layer that projects feature vectors to RGB colors and fromRGB does the reverse; both use 1×1 convolutions. When training the discriminator, we feed in real images that are downsampled to match the current resolution of the network. During a resolution transition, we interpolate between two resolutions of the real images, similarly to how the generator output combines two resolutions.

(Karras et al, 2017)

T

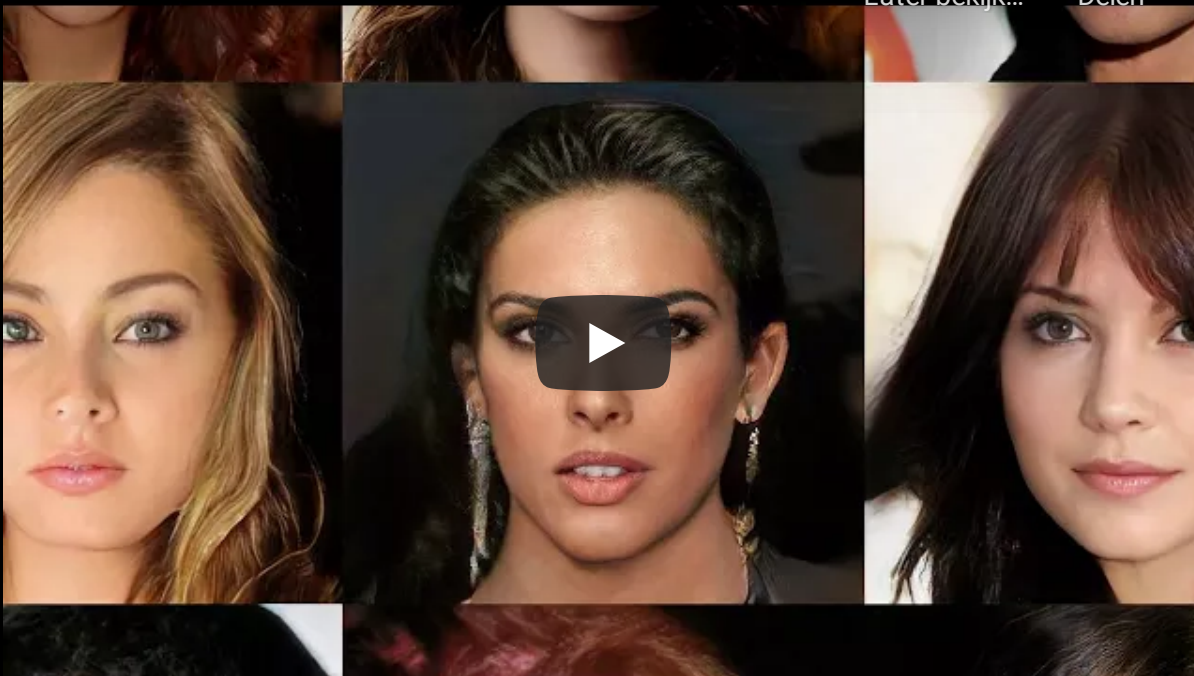
Progressive Growing of GANs for Improved ...



Later bekijk...



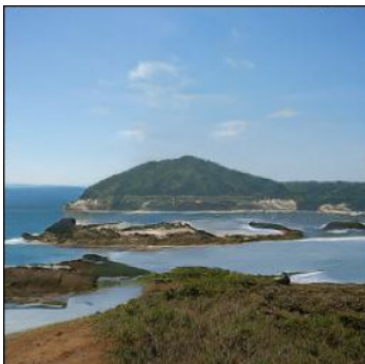
Delen



(Karras et al, 2017)

BigGANs

Self-attention GANs as baseline (Zhang et al, 2018) + Hinge loss objective (Lim and Ye, 2017; Tran et al, 2017) + Class information to g with class-conditional batchnorm (de Vries et al, 2017) + Class information to d with projection (Miyato and Koyama, 2018) + Half the learning rate of SAGAN, 2 d -steps per g -step + Spectral normalization for both g and d + Orthogonal initialization (Saxe et al, 2014) + Large minibatches (2048) + Large number of convolution filters + Shared embedding and hierarchical latent spaces + Orthogonal regularization + Truncated sampling + (quite a few other tricks)



(Brock et al, 2018)



The 1000 ImageNet Categories inside of Bi...



Later bekijk...



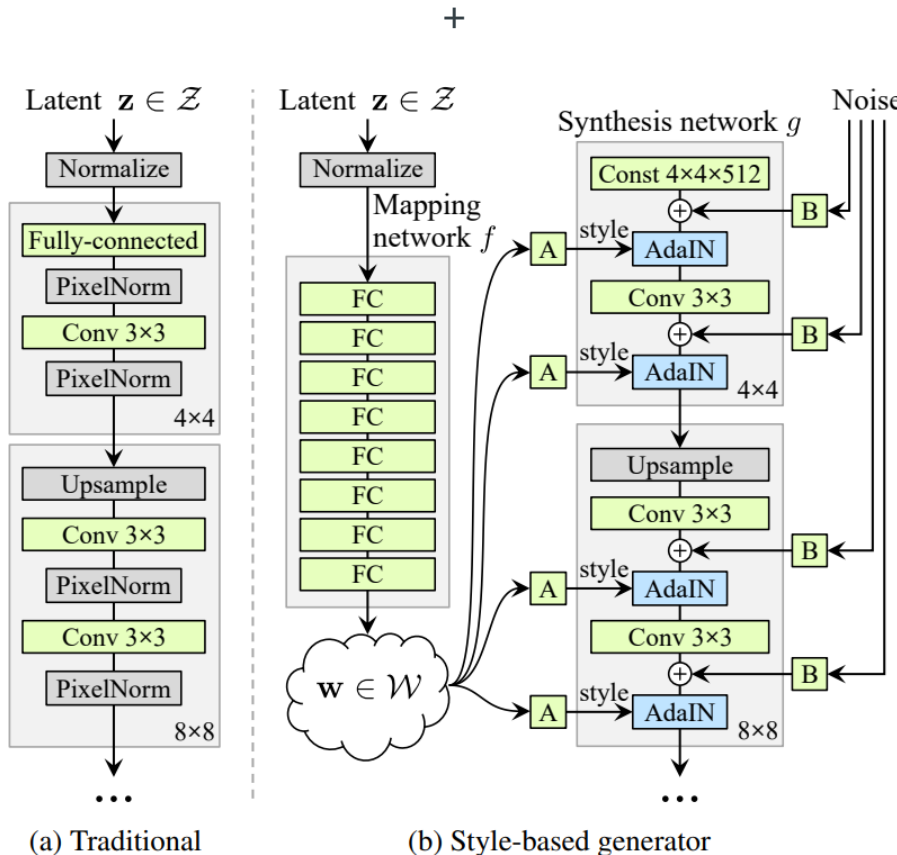
Delen



(Brock et al, 2018)

StyleGAN (v1)

Progressive GANs as baseline (Karras et al, 2017) + Non-saturating loss instead of WGAN-GP + R_1 regularization (Mescheder et al, 2018) + (quite a few other tricks)



T

A Style-Based Generator Architecture for G...



Later bekijk...



Delen

Coarse styles
 $(4^2 - 8^2)$



Middle styles
 $(16^2 - 32^2)$

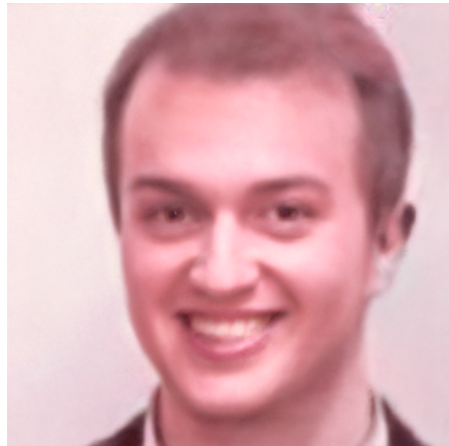


Fine styles
 $(64^2 - 1024^2)$



(Karras et al, 2018)

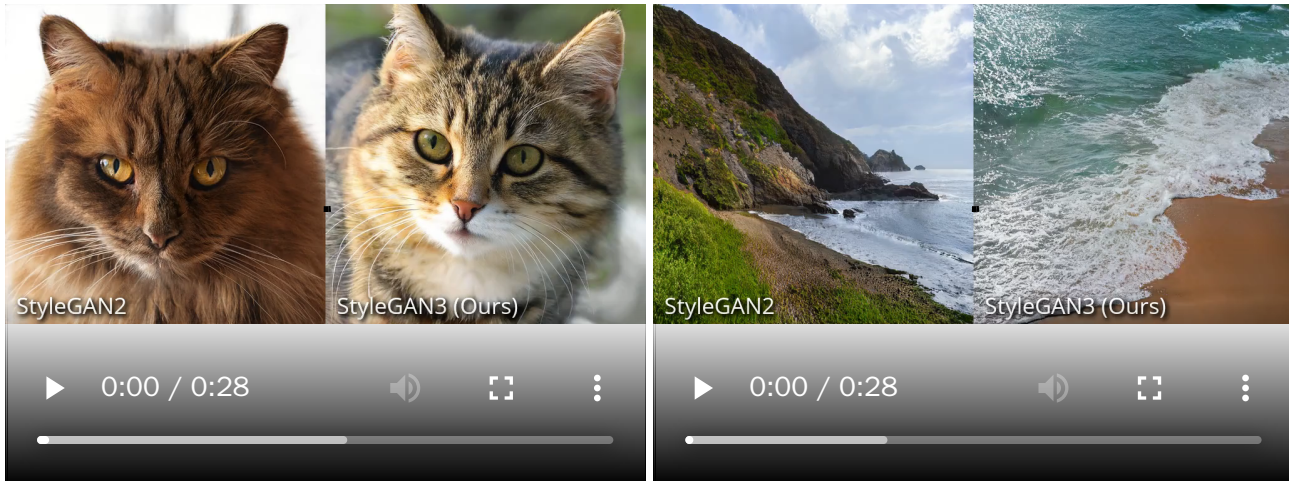
The StyleGAN generator *g* is so powerful that it can re-generate arbitrary faces.







StyleGAN (v2, v3)



(Karras et al, 2019; Karras et al, 2021)

VQGAN

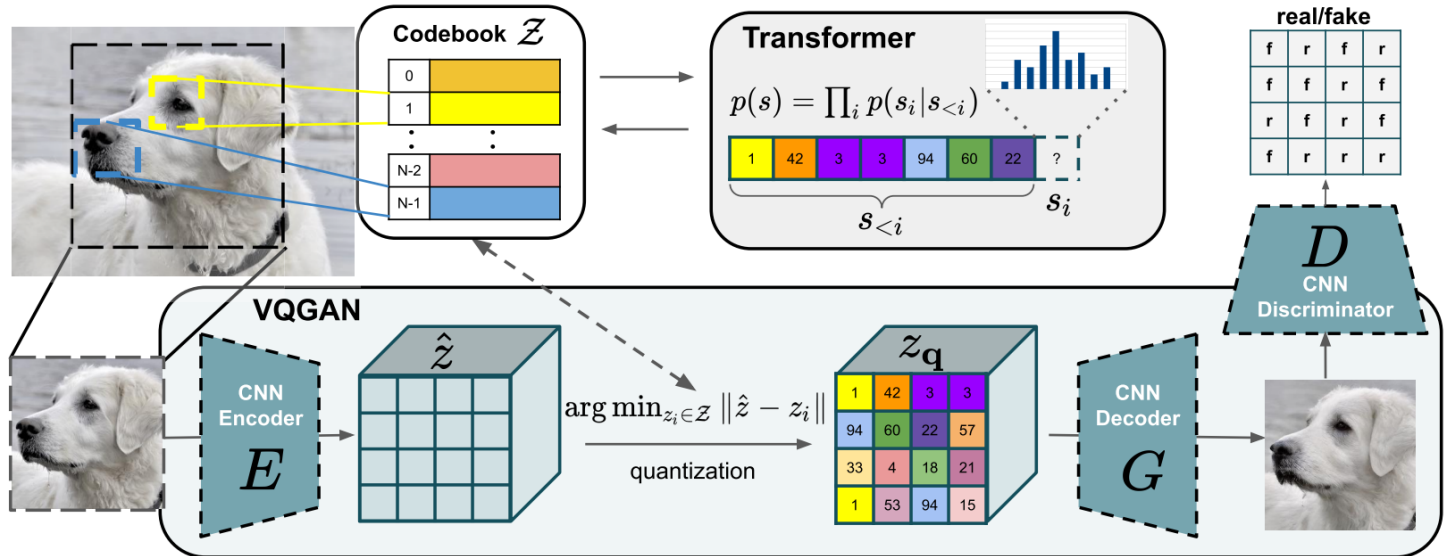


Figure 2. Our approach uses a convolutional VQGAN to learn a codebook of context-rich visual parts, whose composition is subsequently modeled with an autoregressive transformer architecture. A discrete codebook provides the interface between these architectures and a patch-based discriminator enables strong compression while retaining high perceptual quality. This method introduces the efficiency of convolutional approaches to transformer based high resolution image synthesis.

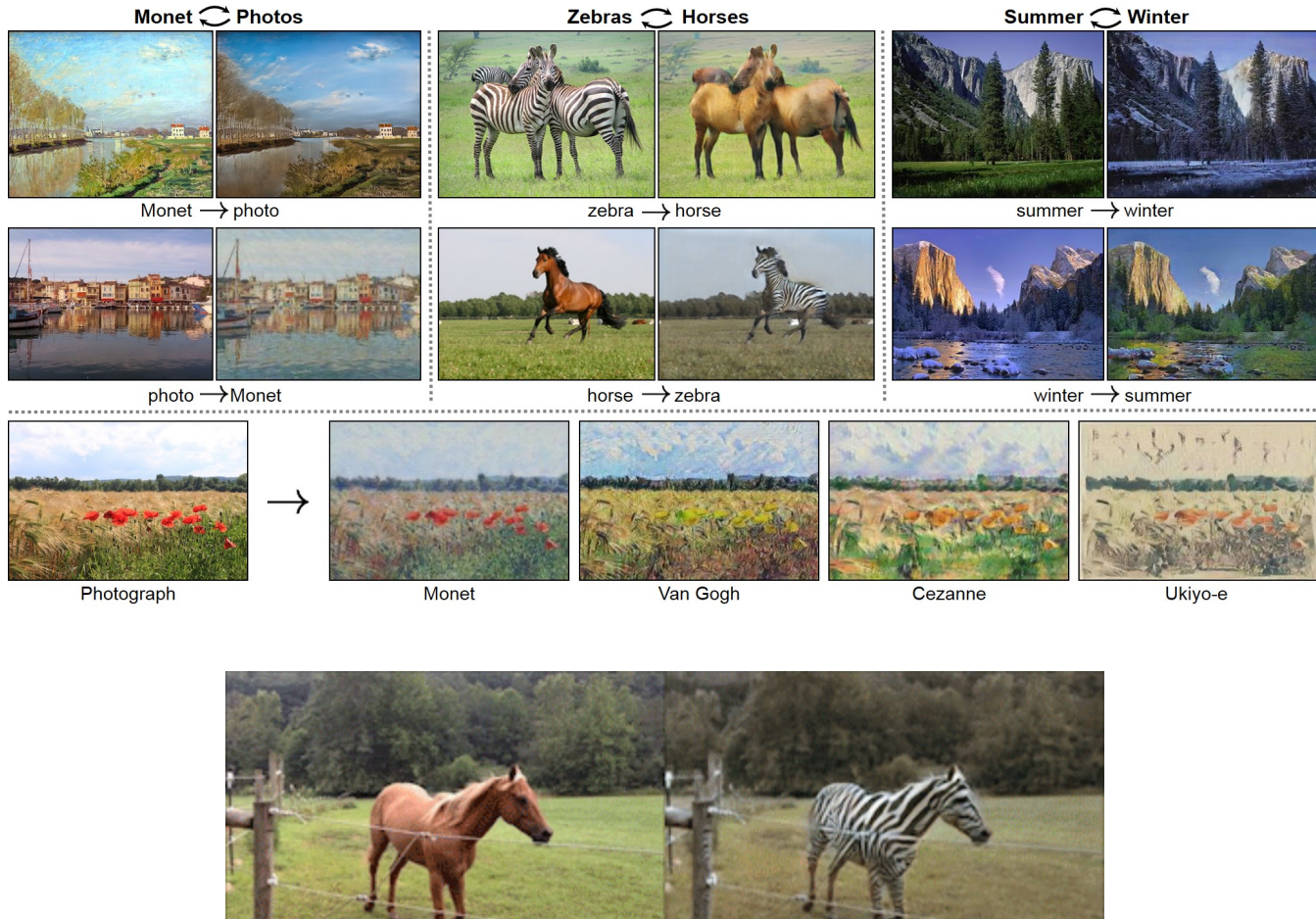
(Esser et al, 2021)



(Esser et al, 2021)

Applications

Image-to-image translation



CycleGANs (Zhu et al, 2017)



High-Resolution Image Synthesis and Sem...



Later bekijk...



Delen



High-resolution image synthesis (Wang et al, 2017)



GauGAN: Changing Sketches into Photoreal...



Later bekijk...



Delen



GauGAN: Changing sketches into photorealistic masterpieces (NVIDIA, 2019)

G

Introduction of GauGAN2 by NVIDIA Research



Link kopier...



GauGAN2 (NVIDIA, 2021)

Living portraits / deepfakes

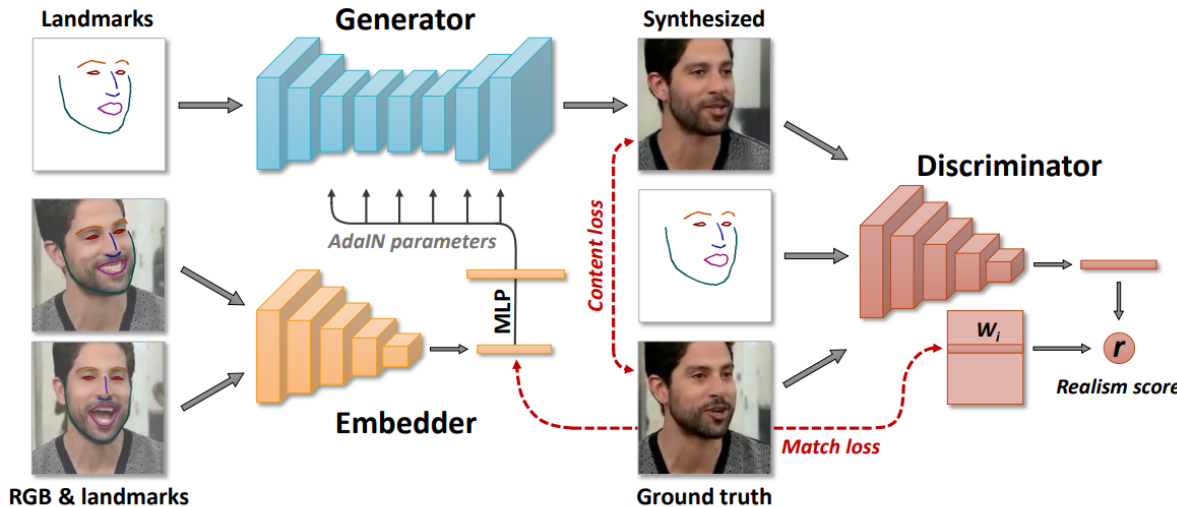


Figure 2: Our meta-learning architecture involves the embedder network that maps head images (with estimated face landmarks) to the embedding vectors, which contain pose-independent information. The generator network maps input face landmarks into output frames through the set of convolutional layers, which are modulated by the embedding vectors via adaptive instance normalization. During meta-learning, we pass sets of frames from the same video through the embedder, average the resulting embeddings and use them to predict adaptive parameters of the generator. Then, we pass the landmarks of a different frame through the generator, comparing the resulting image with the ground truth. Our objective function includes perceptual and adversarial losses, with the latter being implemented via a conditional projection discriminator.

Few-Shot Adversarial Learning of Realistic Neural Talking Head Models
(Zakharov et al, 2019)



Excerpt from Few-Shot Adversarial Learnin...

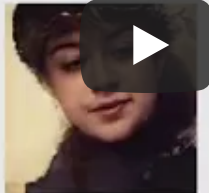


Later bekijk...



Delen

Living portraits



Few-Shot Adversarial Learning of Realistic Neural Talking Head Models
(Zakharov et al, 2019)

Captioning



a tennis player gets ready to return a serve



two men dressed in costumes and holding tennis rackets



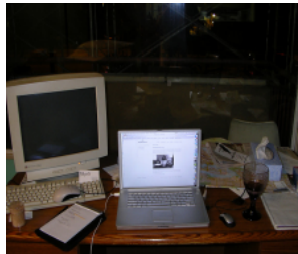
a tennis player hits the ball during a match



a male tennis player in action on the court



a man in white is about to serve a tennis ball



a laptop and a desktop computer sit on a desk



a person is working on a computer screen



a cup of coffee sitting next to a laptop



a laptop computer sitting on top of a desk next to a



a picture of a computer on a desk

(Shetty et al, 2017)

Text-to-image synthesis

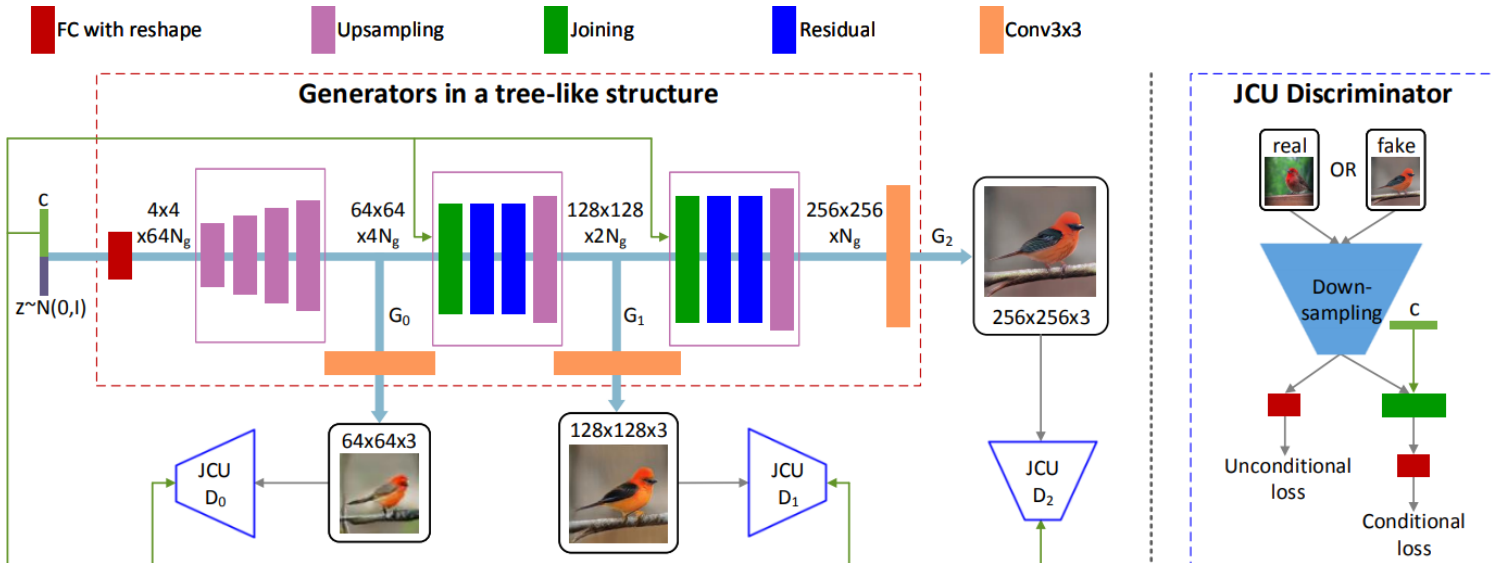


Fig. 2: The overall framework of our proposed StackGAN-v2 for the conditional image synthesis task. c is the vector of conditioning variables which can be computed from the class label, the text description, etc.. N_g and N_d are the numbers of channels of a tensor.

(Zhang et al, 2017)

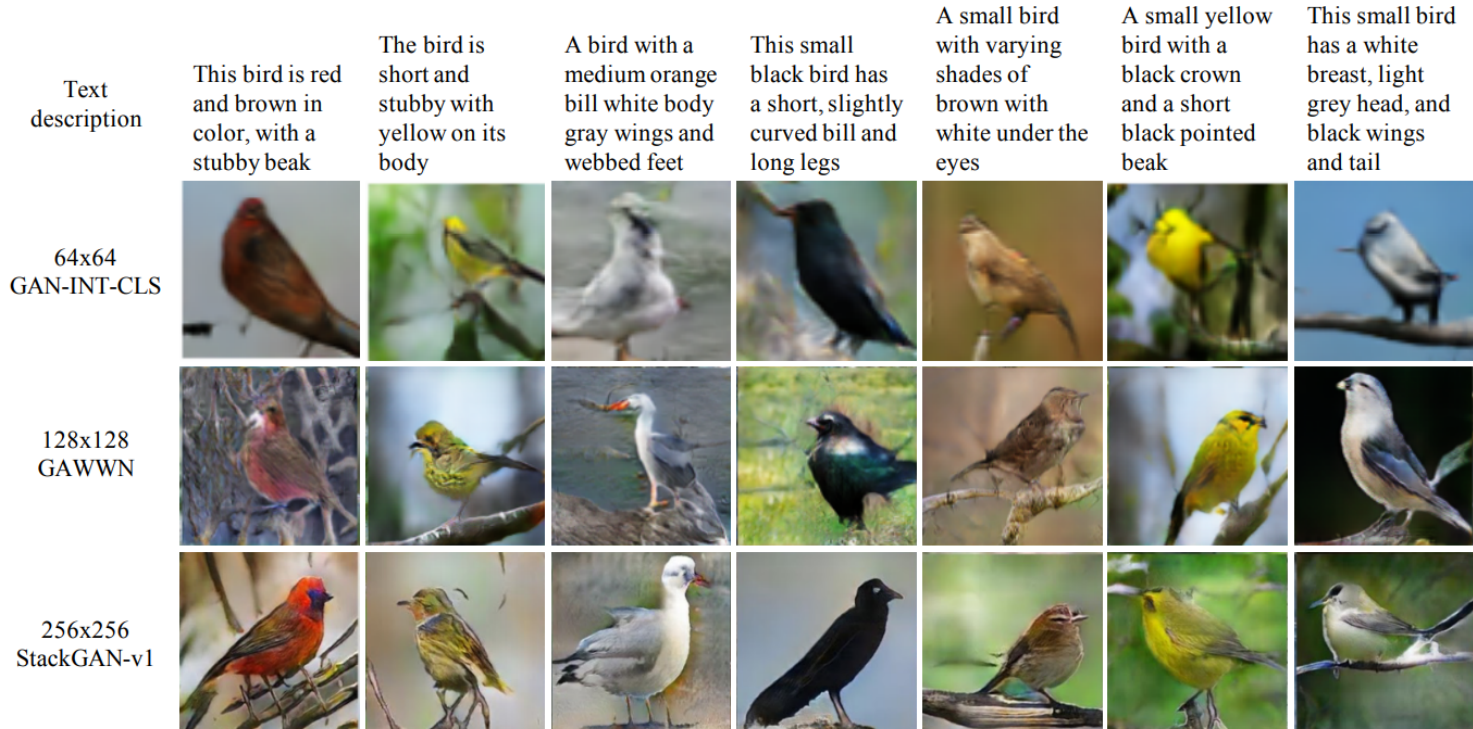


Fig. 3: Example results by our StackGAN-v1, GAWWN [29], and GAN-INT-CLS [31] conditioned on text descriptions from CUB test set.

(Zhang et al, 2017)

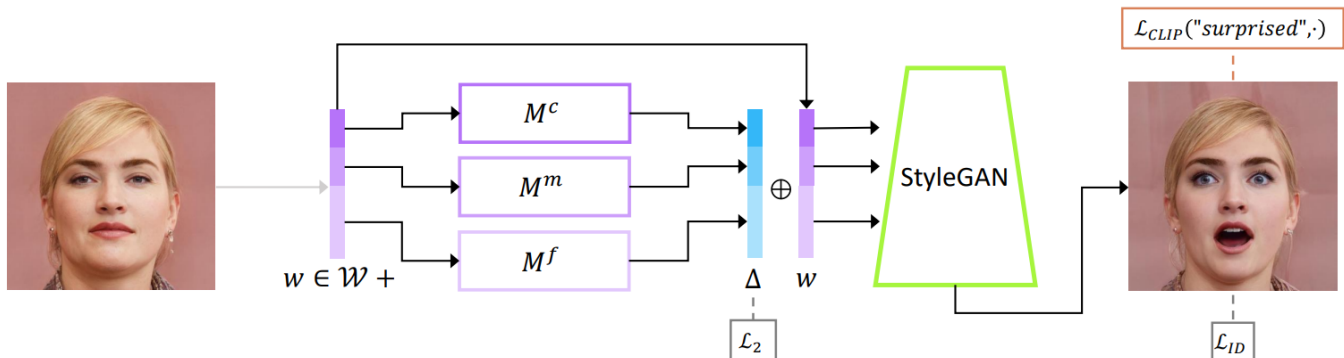
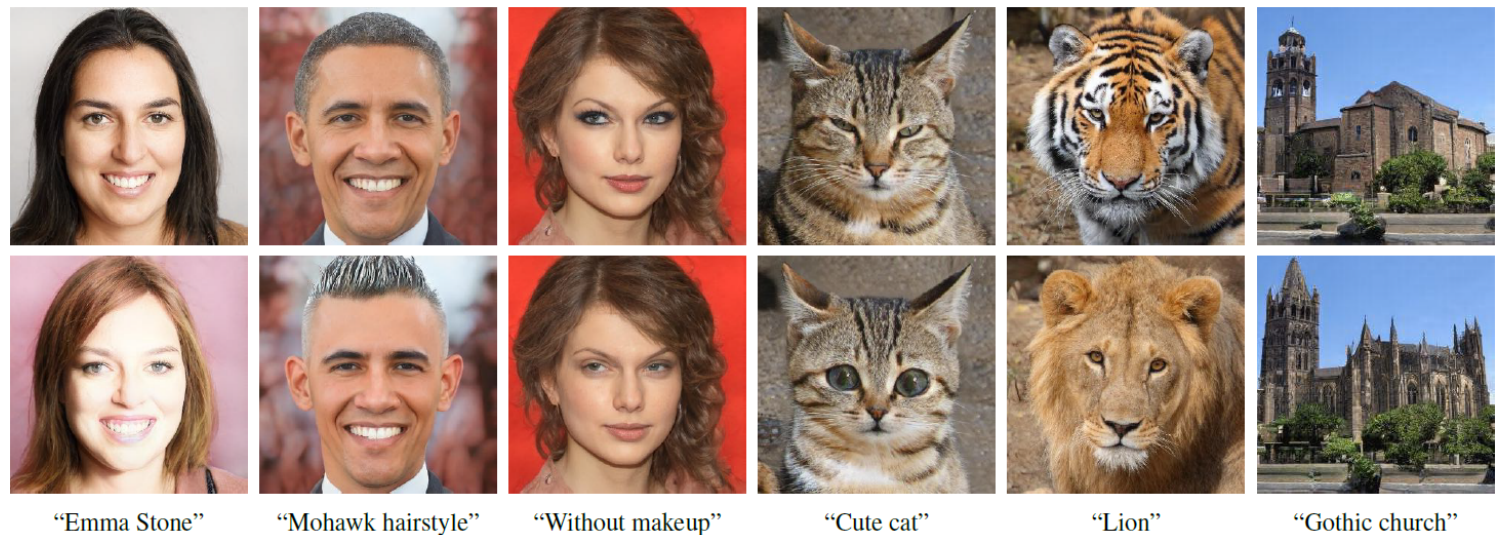


Figure 2. The architecture of our text-guided mapper (using the text prompt “surprised”, in this example). The source image (left) is inverted into a latent code w . Three separate mapping functions are trained to generate residuals (in blue) that are added to w to yield the target code, from which a pretrained StyleGAN (in green) generates an image (right), assessed by the CLIP and identity losses.



StyleCLIP (Patashnik et al, 2021)

Music generation

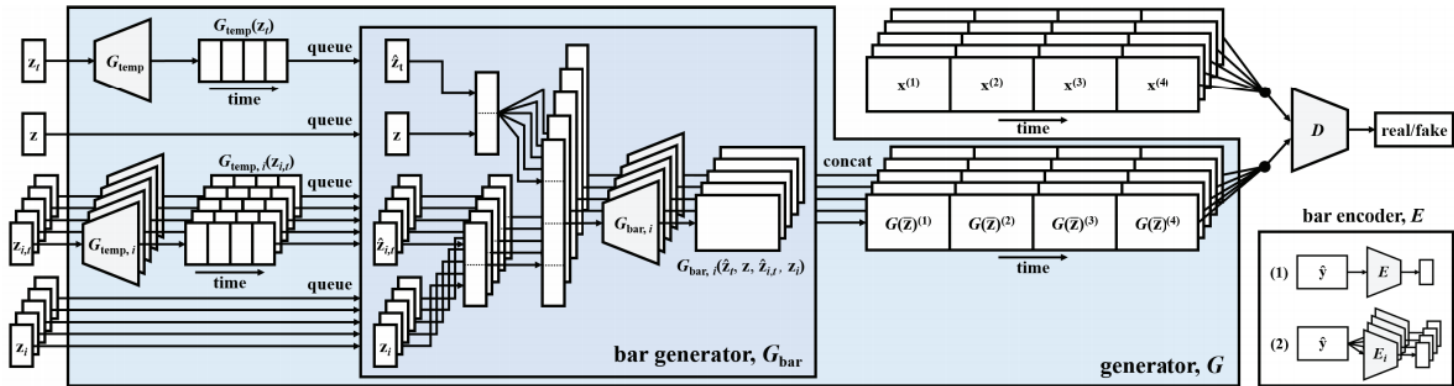


Figure 5: System diagram of the proposed MuseGAN model for multi-track sequential data generation.

▶ 0:00 / 3:15 🔍

MuseGAN (Dong et al, 2018)

Accelerating scientific simulators

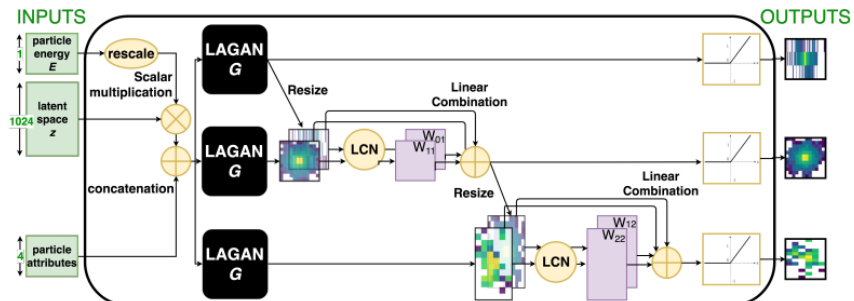


Figure 8.37: Composite conditional CaloGAN generator G , with three LAGAN-like streams connected by attentional layer-to-layer dependence.

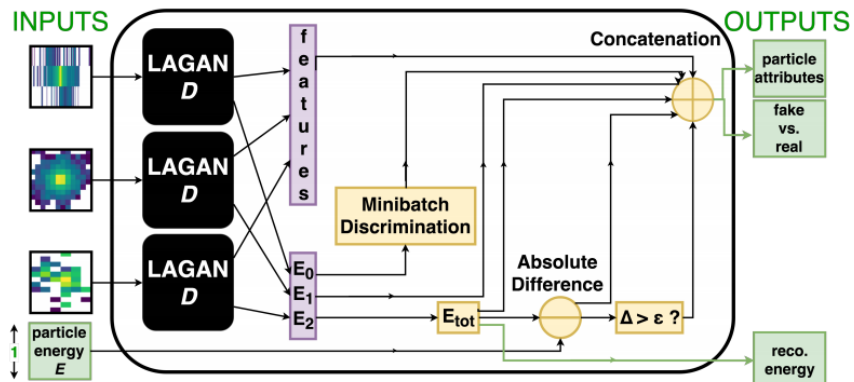
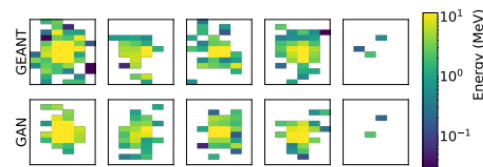
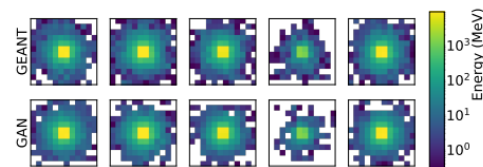
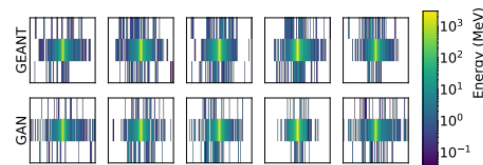


Figure 8.38: Composite conditional CaloGAN discriminator D , with three LAGAN-like streams and additional domain-specific energy calculations included in the final feature space.



Learning particle physics (Paganini et al, 2017)

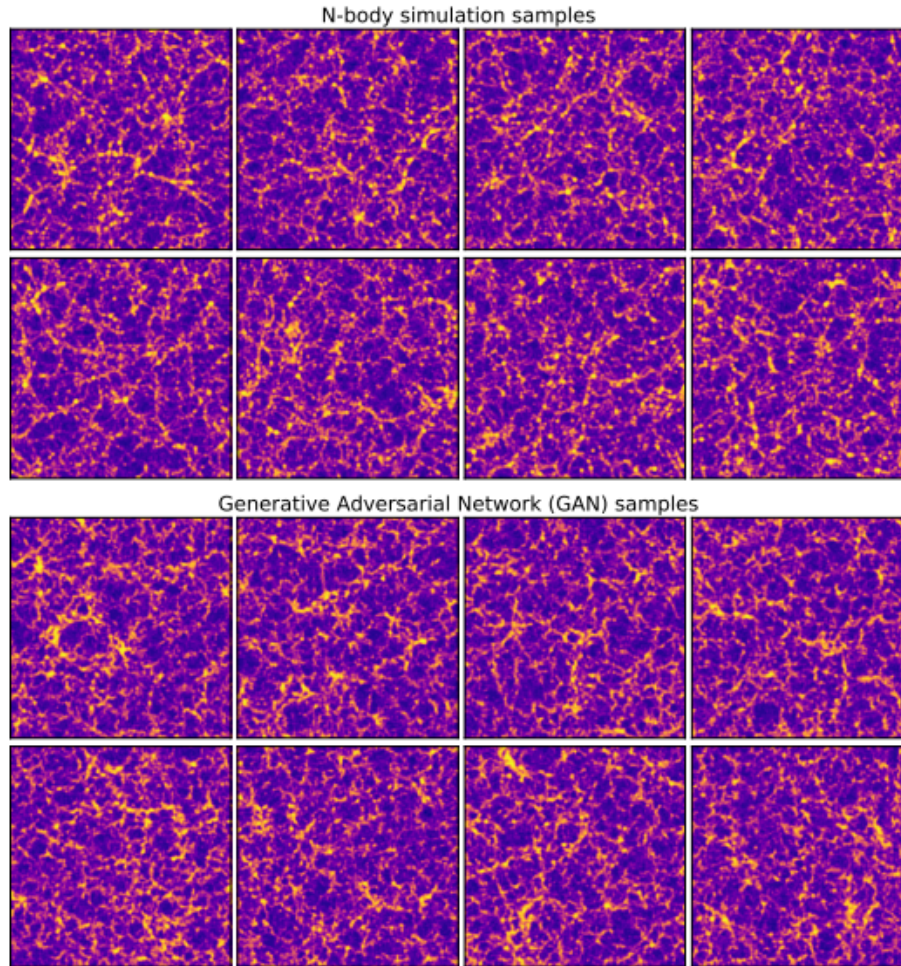


Figure 1: Samples from N-body simulation and from GAN for the box size of 500 Mpc. Note that the transformation in Equation 3.1 with $a = 20$ was applied to the images shown above for better clarity.

Learning cosmological models (Rodriguez et al, 2018)

The end.